IEEE Photonics Journal
An IEEE Photonics Society Publication

Open Access

Rolling OFDM for Image Sensor Based Optical Wireless Communication

Volume 11, Number 4, August 2019

Huy Nguyen
Minh Duc Thieu
Trang Nguyen
Yeong Min Jang

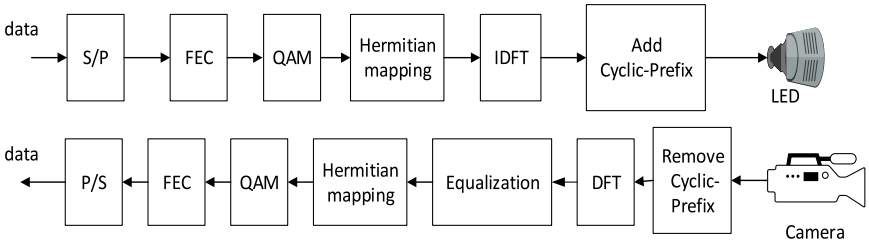

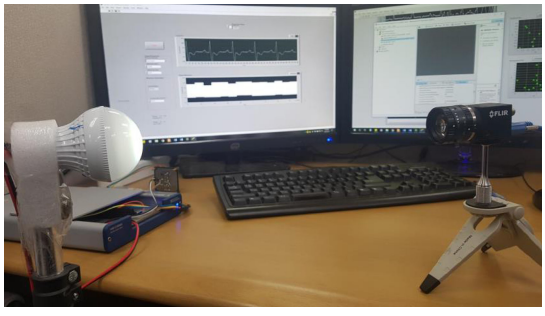

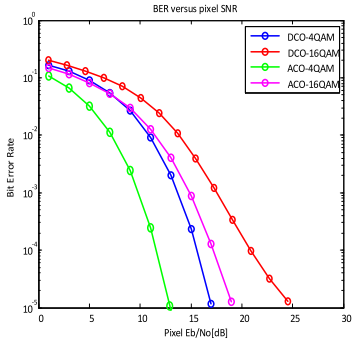

DOI: 10.1109/JPHOT.2019.2926394

Rolling OFDM for Image Sensor Based Optical Wireless Communication

Huy Nguyen, Minh Duc Thieu, Trang Nguyen, and Yeong Min Jang

Department of Electronics Engineering, Kookmin University, Seoul 136-702, South Korea

DOI:10.1109/JPHOT.2019.2926394

Manuscript received May 21, 2019; revised June 23, 2019; accepted June 28, 2019. Date of publication July 3, 2019; date of current version July 19, 2019. This work was supported by the Ministry of Science and ICT, Korea, under the Information Technology Research Center support program (IITP-2018-0-01396) supervised by the Institute for Information & communications Technology Promotion. Corresponding author: Yeong Min Jang (e-mail: yjang@kookmin.ac.kr).

This paper has supplementary downloadable material available at http://ieeexplore.ieee.org.

Abstract: Orthogonal frequency-division multiplexing (OFDM) is a digital multicarrier modulation scheme that is employed in broadband wired and wireless communication as an effective solution with inter-symbol interference caused by a multipath channel. In light fidelity, the OFDM waveform is well-known and frequently implemented; however, the use of such technology with optical camera communication (OCC) is novel. This paper presents the one-dimensional OFDM OCC system. The modulation scheme based on OFDM uses a rolling-shutter effect to transmit data at a high rate. Based on theoretical and experimental validation, we propose a simple system design with various technical details such as system architectures and theoretical analyses of the link budget.

Index Terms: Optical camera communication, OCC, OFDM, optical-OFDM, 1D-OFDM, rolling OFDM.

1. Introduction

Demand for high-rate communication persists, encouraging technological advancements to increase efficiency and improve overall performance. Wireless communication demonstrates superiority over wired communication, as it is easier to install and enables ubiquitous data transmission without depending on wires. Such advancements have been critical to developing mobile networks. Wireless Technologies based on Radio Frequencies (RFs) are gradually exhausting their resources, and in order to improve data speed, we must use a higher frequency band. Many researchers have been working to develop the fifth generation of cellular mobile communications (5G) in the millimeter wave band, which promises to render a high-speed system (1–10 Gbps). However, it is important to note that the higher frequency comes with potentially harmful side effects to human health.

Studies on the use of visible light for data transmission are also becoming more prevalent with new viable candidates including Visible Light Communication (VLC), Optical Wireless Communication (OWC)/Optical Camera Communication (OCC), each of which may replace Radio Frequency Communication. The advances of VLC or OWC/OCC over RF communication can be summarized as follows:

- Light waves do not negatively affect human health if supported by dimming and non-flicker methods. Depending on research results with human subjects, [1] demonstrates that the optical modulation frequency up to 200 Hz can be considered without affecting human eyes.

- The bandwidth of visible light is more than 1000 times the RF bandwidth.
- Visible light waves are more cost-efficient. Also, visible light is available in light infrastructures on streets and vehicles, which decreases the cost of implementing VLC and OWC/OCC systems in comparison to implementing RF.

Hence, many companies are investing the majority of their budgets in researching this novel technology. The OWC system has been overviewed in IEEE 802.15 and IEEE 802.11 tutorials [2]. In [2], the wide range of protocol complexity acceptance and the uniqueness of OWC have also been accepted. The IEEE 802.15.7m Task Group (TG7m) has classified the system into four categories:

- Existing Visible Light Communication (VLC) modes available in IEEE 802.157-2011 standard [3].
- Optical Camera Communication (OCC): baseband modulation techniques use cameras or image sensors to receive signals from a light source.
- LED Identification (LED-ID): communication techniques using photodiodes at low speeds with data rates below 1Mbps at the physical layer.
- High-speed Light Fidelity (Li-Fi): high-rate photodiode modulation techniques with data rates exceeding 1Mbps at the physical layer. Optical-Orthogonal Frequency-Division Multiplexing modulations are the essential modulation utilized in Li-Fi technologies.

Unlike VLC and Li-Fi technologies using photodiodes, Optical Camera Communication technology employs a camera as the detector to receive data. [4], [5] demonstrate that the performance of OCC systems depends on the type of camera. In the market, Global Shutter and rolling-shutter camera are two popular cameras for this setup. With the Global Shutter Camera, OCC performance is primarily decided by the camera frame rate, which determines whether the sampling rate satisfies the Nyquist sampling requirement. With the rolling-shutter camera, the sampling rate is also dependent on both the camera frame rate and the rolling rate of the camera.

The Orthogonal Frequency-Division Multiplexing (OFDM) is a modulation method for digital data encoding on multiple carrier frequencies. It is an essential technique in high-speed communication because the bandwidth is divided into the orthogonal sub-carrier to eliminate the distortion caused by Inter-Symbol Interference (ISI). By using the Fourier Transform method, the sub-carrier in the OFDM system can overlap on each other without affecting signal performance. Additionally, the Cyclic-Prefix is added to the OFDM symbol to combat the distortion.

In [6], we proposed 2-Dimensional Orthogonal Frequency-Division Multiplexing (2D-OFDM) in Screen OCC systems. 2D-OFDM focus on using Asynchronous-Quick-Link (A-QL) code to receive the 2D-OFDM waveform in Screen OCC systems. The disadvantage of 2D-OFDM is the transmission distance, which works reliably at 3m-distance [6]. This paper focuses on 1-Dimensional Orthogonal Frequency-Division Multiplexing that depends on the rolling effect of a rolling-shutter camera. In this paper, we show the SNR measurement to make sure that the proposed scheme can achieve Bit Error Rate of 10^{-4} at 20 m if we control the exposure time suitably. Besides that, Rolling OFDM scheme is easy to set up in Tx side than 2D-OFDM scheme due to only using LED while 2D-OFDM scheme needs big-screen to transmit.

The remainder of this paper consists of four sections which are structured as Follows: In Section 2, we introduce the principles of the OFDM scheme and highlight technique contributions. Section 3 recalls the fundamentals of OFDM and the OFDM methods utilized in the OCC system. Section 4 presents the implementation results of the rolling-OFDM system; the scheme architecture with its contributions are illustrated in Section 2. The final section concludes the paper.

2. Our Contributions

A survey on the contribution of OFDM techniques on RF and LiFi systems is an initial, but it is an indispensable stage to our contributions among many research directions. The benefits of OFDM technology to show an overview of the advantages of OFDM technique with RF system and LiFi system for readers is shown in Subsection 2.1. In Subsection 2.2, the technical contributions of Rolling OFDM will be discussed to highlight our contributions.

2.1 Benefits of OFDM

Orthogonal Frequency-Division Multiplexing (OFDM) was introduced by Bell Lab in 1966 [7] but only reached sufficient maturity for standardization and employment in the 1990s. By using multi-carriers, the OFDM scheme has many advantages compared to a single-carrier modulation scheme. The OFDM system is a particular form of Frequency-Division Multiplexing (FDM), dividing the high bit rate stream into lower bitrate streams and simultaneously transmitting all streams through orthogonal subcarriers. Hence, the bandwidth is used more effectively than in a traditional FDM system. The use of multicarrier modulation for OFDM has improved the primary disadvantage of wideband communication by eliminating ISI. ISI is a signal distortion caused by multipath fading, which causes symbols to interfere with one another. This interference is especially dangerous with broadband systems where the spreading time of the system is much larger than the symbol interval. By splitting the bandwidth, the OFDM system can mitigate the ISI by adding a Cyclic Prefix (CP) to the OFDM symbol, augmenting it enough to mitigate the negative impact of ISI completely. However, the CP interval does not carry a signal; therefore, the length of the CP must be carefully selected to balance ISI reduction effective performance.

Light Fidelity (Li-Fi) is a wireless communication technology that uses light to transmit data, which allows Li-Fi to offer several advantages, such as higher bandwidth, high transmission speeds, and the ability to function in areas susceptible to electromagnetic interference. Due to the request data rate increase in Li-Fi systems, unwanted effects have been revealed for single-carrier modulation (SCM) such as nonlinear signal distortion at the LED terminal and ISI caused by frequency selectivity in OWC. Therefore, MCM has been researched and applied to Li-Fi systems to increase performance. One of the most commonly implemented methods of MCM in Li-Fi systems is OFDM [8]. If the bandwidth is divided into many orthogonal subcarriers, the bandwidth of each signal is smaller than the coherence bandwidth, and the sub-channel is flat fading compared to the frequency selective fading in an SCM system.

2.2 Technical Contributions of Rolling-OFDM

Throughout this study, we proposed the new scheme applying OFDM in OCC system based on rolling effect. Discrete Fourier Transform(DFT) and Discrete Wavelet Transform (DWT) are two main approaches which employed for the generation of subcarriers. The DFT was widely applied for the OFDM techniques, but a practical demonstration showed that the DWT shown more potentials than DFT.

In my best of knowledge, the application of rolling shutter effect to OFDM for OCC system is still very little. Applying the OFDM technique to OCC system based on rolling shutter faces many challenges. The rolling shutter effect is easy to apply with On-Off Key (OOK) modulation, but applying OFDM technique in intensity modulation/direct detection(IM/DD) modulations are extremely difficult. How to choose the exposure time and packet interval to the decoder with each image at the receiver side? How to optimal but decodable packet design? Rolling OFDM is not a novel idea; however, some outstanding contributions of the proposed system can be represented as the following:

- Frame rate variation support: In an OCC system, frame rate variation is dangerous. In most cases, people believe that the frame rate of the camera is defined (e.g., 30 fps or 1000 fps). However, in reality, every camera has its own level of frame rate varies depending on its technical parameter, which cannot be predicted, increasing how difficult it is to synchronize Tx and Rx. By using the Sequence Number, any receiver that has a frame rate higher than the packet rate of the transmitter can decode data easily by checking the value of the Sequence Number.
- Data merger algorithm: The Sequence Number can not only help frame rate variation but can also improve the performance of the system by using the data merger algorithm. Our idea is to combine the packages into a complete data sequence in the correct order.

- Detection of missing packets: If the length of the Sequence Number surpasses a certain point, every missing packet can be detected easily by comparing two Sequence Numbers of two adjacent images captured by the camera.
- The proposed scheme can reduce ISI, which causes two cases: Multipath and blur phenomenon. In the real environment, the light source can be reflected from water, terrestrial object. From that, the camera receives many versions of signal causing ISI. The blur phenomenon also is the leading cause of ISI; one pixel affects another pixel, then one OFDM symbol will be interfered by another symbol causing ISI. With adding a cyclic prefix, ISI will be mitigated if the maximum delay time is less than the guard interval.
- In an OCC system, the trouble of complex noise (blur image, interference, irregular attenuation) is difficult within the time domain but can be easily resolved in the frequency domain by ignoring the DC-component.
- Moreover, the complete OFDM symbol with creation and post-processing at Tx are shown as follows:
  - The new design of Physical Protocol Data Unit Format for rolling-OFDM systems (presented in this paper).
  - Effective design of pilots and channel equalization.

3. Principle and Related Works

3.1 1-D OFDM Fundament

The Fourier Transform helps us overview the relationship between the time domain and the frequency domain. There are many versions of the FT, and each operates depending on the particular circumstances of the work. The conventional Fourier Transform relates to continuous signals. However, the continuous signal is difficult to process because it is not limited to either the frequency domain or time domain. If signals are sampled, signal processing is made easier. Hence, to avoid this disadvantage, the Discrete Fourier Transform (DFT) is widely used in signal processing. DFT is a variation of the Fourier Transform in which the signals are sampled in both the time domain and frequency domain.

The definition of Discrete-Fourier Transform (DFT) is well-known and represented as a periodic transform:

$$X[k] = \sum_{n=0}^{N-1} x[n].e^{-\frac{2\Pi.i}{N}.k.n} \text{ with } k = 0, 1, 2, \ldots, N-1 \tag{1}$$

Meanwhile, the Inverse-Discrete Fourier Transform (IDFT) is defined as follows:

$$x[n] = \frac{1}{N} \sum_{k=0}^{N-1} X[k].e^{2\Pi.i.\frac{k}{N}n} \text{ with } n = 0, 1, 2, \ldots, N-1 \tag{2}$$

The orthogonality between the subcarriers can be described as follows:

$$\sum_{k=0}^{N-1} \cos\left(\frac{2\Pi kn}{N}\right) \cos\left(\frac{2\Pi km}{N}\right) = \delta(n-m) \tag{3}$$

Taking advantage of the orthogonality of IDFT elements, we can use the IDFT block to make orthogonal signals in OFDM, as shown in Fig. 1.

3.2 Related Works

Depending on the orthogonality of the Fourier Transform (FT), the FT has been proposed instead to the banks of sinusoidal in 1966. In 1969, the CP was proposed as an addition to OFDM systems to

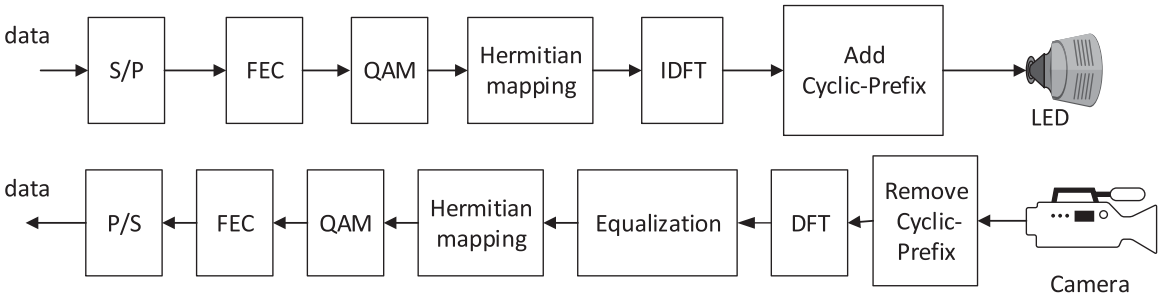

Fig. 1. Block diagram of architecture of rolling shutter-OFDM system.

TABLE 1
Comparison of OFDM Techniques (Refer to [6])

	ACO-OFDM	DCO-OFDM	DWT-OFDM
Modulation	QAM	QAM	QAM/PAM
MCM method	Discrete Fourier Transform	Discrete Fourier Transform	Discrete Wavelet Transform
Complex-real conversion	Odd subcarriers Hermitian mapping	All subcarriers Hermitian Mapping	Direct mapping for PAM, Dual-modulator for QAM
Modulation PAR and Clipping	Bias-clipping to the-top	Balanced doubled-side clipping	Lower PAPR, No clipping
Principle Characteristic	Better power efficiency by the use of half subcarriers	Better bandwidth efficiency by the use of all subcarriers	Same bandwidth efficiency as DCO-OFDM (DCO-OFDM applies to the complex number but needs Hermitian mapping)
Implementation perspective	Lower data rate but more stable performance with noise.	Higher data rate but NULL carriers critically needed.	Half of the sub bands used, PAM modulation limited. Less implemental complexity
Cyclic Prefix	Need	Need	No need

combat ISI. In 1980, researchers also began to apply OFDM for practical wireless communication.

$$X(\omega) = \sum_{i=-\infty}^{\infty} x[n]e^{-i\omega n} \tag{4}$$

With an OWC system, or more particularly an OCC system, the signal is a light source, and the non-negative waveform is a mandatory condition. Therefore, the waveform needs to be pre-processed before going to the IDFT block. Currently, Asymmetrically Clipped Optical-OFDM (ACO-OFDM) and DC-biased Optical-OFDM (DCO-OFDM) are two developed technologies for Li-Fi systems. However, in comparison to the Fourier Transform, the wavelet transform offers many advantages such as no redundancy in CP, reduction of sub-channel interference, and higher spectral separation. Wavelet OFDM has just been standardized by the IEEE Standard Association (Wavelet Transform is the main topic of IEEE 1901 for the power line communication standard). Table 1 briefly compares the given techniques. In [9], the theoretical performance of wavelet OFDM is presented. The superiority of wavelet OFDM compared to conventional OFDM is demonstrated. [10] gives that the wavelet OFDM has spectral efficiency, suppression of side-lobes and bit error rate performance beyond that of DCO-OFDM. [11] introduces the wavelet packet applications to OWC systems and demonstrates that the PAPR of wavelet OFDM is smaller and has better robustness in dealing with channel imperfection.

3.2.1 DCO-OFDM: In [12], [13], it is exhibited that DCO-OFDM are preferred over ACO-OFDM for IM/DD systems by industrial companies and research institutes as PureLiFi of the United Kingdom and Fraunhofer Heinrich Hertz Institute of Germany because the DCO-OFDM scheme provides better bandwidth efficiency than the ACO-OFDM scheme when all subcarriers are used rather than just odd subcarriers. To ensure the unipolar property of the light source waveform, DCO-OFDM requires a post-processing procedure. The most straightforward post-processing procedure can be executed by adding DC-bias to achieve a non-zero waveform within the range of LED operation. Despite the better bandwidth efficiency, the BER performance of DCO-OFDM is worse than that of ACO-OFDM due to the addition of DC-bias.

Before coming to the IDFT block, the data signal, $X = [X_0, X_1, X_2, \ldots, X_{N-1}]$, must be constrained to have Hermitian symmetry:

$$X_m = X^*_{N-m} \text{ for } 0 \leq m \leq \frac{N}{2} \text{ and } X_0 = X_{N/2} = 0 \tag{5}$$

After the IDFT block, the signal x is a real signal in the time domain. The k^{th} time domain sample of x is shown:

$$x_k = \frac{1}{2} \sum_{m=0}^{N-1} X_m e^{\frac{j2\Pi.k.m}{N}} \tag{6}$$

Despite following this procedure, the signal still has a negative element. We must then add DC-bias to the signal, ensuring that the signal is not complex and non-negative.

3.2.2 ACO-OFDM: In Li-Fi systems, the ACO-OFDM scheme is widely used for a PD-equipped receiver [14], [15]. Unlike DCO-OFDM, ACO-OFDM only uses odd subcarriers to transmit data. In return, its BER performance is more stable than that of DCO-OFDM. Since the NULL data was put onto even subcarriers, the clipping noise falls into the removable carriers at the receiving side, as demonstrated in [16]. Only the odd subcarriers carry data symbols in ADO-OFDM to ensure that the signal after the IDFT is real and non-negative. The input signal to the IDFT, **X**, comprises odd components such as $X = [0, X_1, 0, X_3, 0, \ldots, 0, X_{N-1}]$. After the IDFT block, the resulting real signal is shown as:

$$x_k = -x_{k+\frac{N}{2}} \text{ for } 0 \leq k \leq \frac{N}{2} \tag{7}$$

3.2.3 DWT-OFDM: In order to outline the benefits of the wavelet transform, many studies have been published in various fields, such as power line communication [9], VLC [11], ultra-wideband vehicular communication and optical fiber communication [17]. In [18], the author analyzed the outperformed advantage of DWT compared to DFT. Although DWT specifications in PHY [19] is published by the IEEE Standard Association, the applications of DWT for OCC systems, or more particularly Rolling-camera systems, are not yet as well-known as DFT. Table 1 outlines the advantages of DWT-OFDM compared to ADO-OFDM and DCO-OFDM

4. System Architecture

In this section, we present the technical details of a rolling-OFDM system. Unlike the conventional OFDM in Radio Frequency, instead of feeding the data symbol directly into the IDFT block, each symbol must pass through the Hermitian block. The signal is then fed into the IFFT. The particular purpose of the Hermitian block is that it ensures the output of the IDFT is entirely real.

The following equation illustrates the Hermitian mapping process.

$$X_m = X^*_{N-m} \text{ for } 0 < m < N \text{ and } X_0, X_1, X_2 \ldots..X_{N-1} \tag{8}$$

$$X = [0, X_1, X_2 \ldots.0 \ldots.X^*_2, X^*_1] \tag{9}$$

Operations of another block are described below.

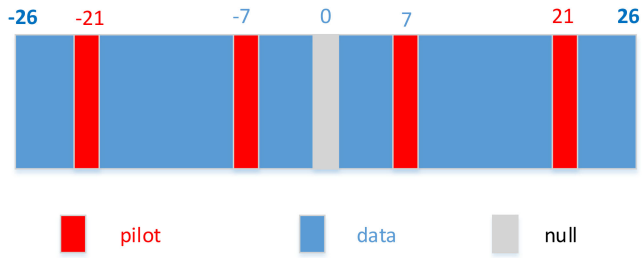

Fig. 2. Example of pilot positions in the OFDM symbol.

4.1 Pilot

To estimate the channel, the pilots need to add the signal before transmissions. Minimal pilot density and pilot location are essential for a system. In [7], the pilot spacing applied for the OFDM symbol was analyzed and simulated.

Let N be the dimension of the OFDM symbol, while Δf is the spacing between subcarriers, so that $N * \Delta f$ is the bandwidth of the OFDM system.

Let τ be the time delay between spatial sampling and T_s be the spatial sampling period. Δp is the maximum spacing of pilots within the OFDM symbol, as shown below.

$$\Delta p \leq \frac{N\Delta f}{2\tau/T_s} \tag{10}$$

The spacing between pilots should be close for acceptable interpolation performance. However, it is noted that the estimation performance is not proportional to the number of pilots. Pilots that are too densely spaced may degrade performance in cases where the channel is over-estimated. Fig. 2 is the sample of pilot positions in the OFDM symbol.

4.2 Equalization

Chanel Equalization is a process of decreasing amplitude distortion and phase distortion. With the equalizer, the channel effect is reduced, thereby improving transmission performance. Then, the equalization method must be discussed to balance the trade-off between the efficiency and complexity of methods [20]. There are two adjacent pilot points: H_0, H_1. The linear interpolation points $H(x)$ between H_0 and H_1 are shown as follows:

$$H(x) = H_0 + (x - x_0).\frac{H_1 - H_0}{x_1 - x_0} \quad \text{with } 0 \leq x \leq 1 \tag{11}$$

$$Y_{equalized} = \frac{Y_{non\_equalized}}{H} \tag{12}$$

Fig. 3 displays the signals before and after the equalizer block.

5. Implementation

5.1 Pixel Eb/No Computation

According to [21], the noise of pixel in CCD/CMOS will be modeled as follow:

$$n \sim N(0, \sigma(s)^2) \tag{13}$$

where s is the value of pixel (the value s ranges from 0 to 255); $\sigma^2(s) = s.a.\alpha + \beta$ with a is mark and space amplitude; α, β are parameters obtained experimentally. The pixel E_b/N_0 can be computed

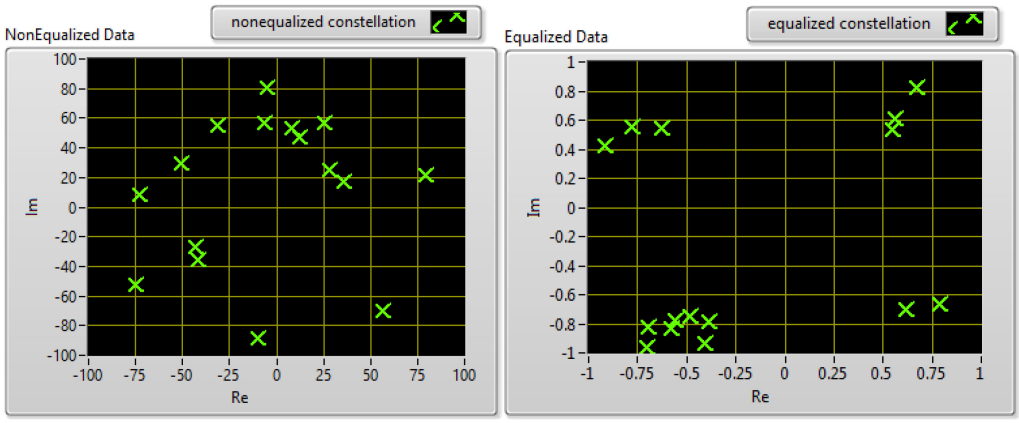

Fig. 3. The signal before and after equalizer block.

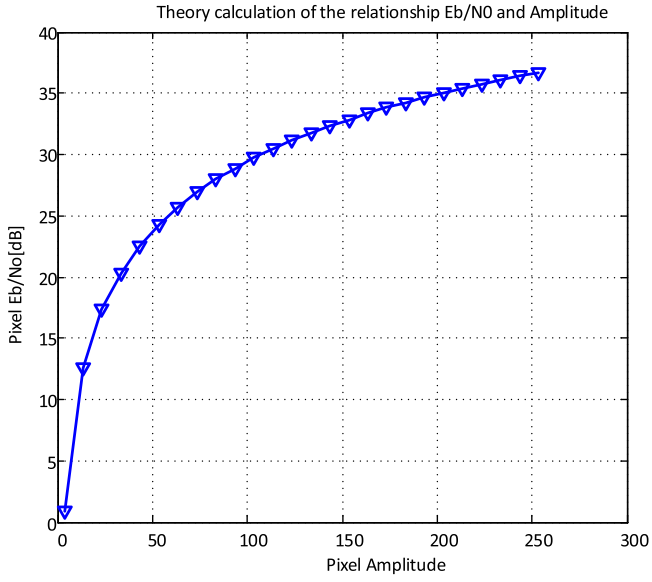

Fig. 4. Simulation of theory calculation Eb/N0.

as follows [21]:

$$Pixel\frac{E_b}{N_0} = \frac{E[s^2]}{E[n^2]} \approx \frac{a^2\Delta}{a.\alpha.\Delta + \beta} \tag{14}$$

where E_b is the bit energy, N_0 is the noise density, s is the value of the pixel, a is mark and space amplitude, $\Delta = T_{exposure}/T_{bit}$ is the ratio of camera exposure time and bit interval, and α and β are relevant parameters. The fit parameters $\alpha = 0.01529$, $\beta = 0.1973$ are estimated and introduced from [21]. From these values, we can estimate the relationship between E_b/N_0 and the pixel value, which is shown in Fig. 4. This relationship is useful in estimating and measuring the pixel SNR ratio and the measurement of pixel value later.

5.2 Experimental SNR Measurement

The measurement of SNR is performed to ensure the SNR satisfaction for the 25 dB required to achieve BER of 10^{-4} in OFDM. In the experiments, an LED (12 DC–2.5 W) was used to measure

Fig. 5. The device for SNR measurement.

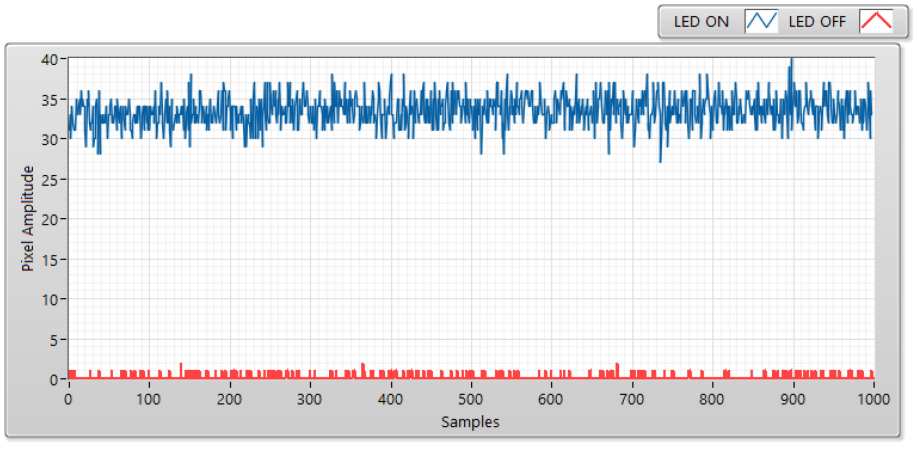

Fig. 6. SNR measurement with rolling shutter camera at 5 m and 50 us exposure time setting.

SNR. Fig. 5 displays the devices used in this experiment. A PointGrey rolling-shutter camera is configured with exposure times at 50 us–500 us and the distance at 5–20 m. An LED (12 DC–2.5 W, 3 cm in diameter) is used in a model of the system.

Figs. 6–9 illustrate the SNR measurement at 5 m, 10, 15, 20 m. The red line is the pixel amplitude when the LED is OFF. It can be considered as background noise. Besides that, the blue line is the pixel amplitude when the LED is ON at different distance. It can be regarded as the signal power of the LED. From that, we can calculate the SNR in dB as following:

$$SNR_{dB} = 20 \log \left(\frac{\sqrt{\frac{1}{n}\sum_{i=0}^{n-1} \left| A\_on_i \right|^2}}{\sqrt{\frac{1}{n}\sum_{i=0}^{n-1} \left| A\_off_i \right|^2}} \right) \tag{15}$$

With A_on is the measured pixel amplitude with LED turned on, A_off is the measured pixel amplitude with LED turned off. n is the number of measured samples.

In the closed position, the received pixel amplitude at the camera will be bigger and vice-versa. Additionally, shutter speed, or exposed time, is the most crucial factor affecting SNR calculation.

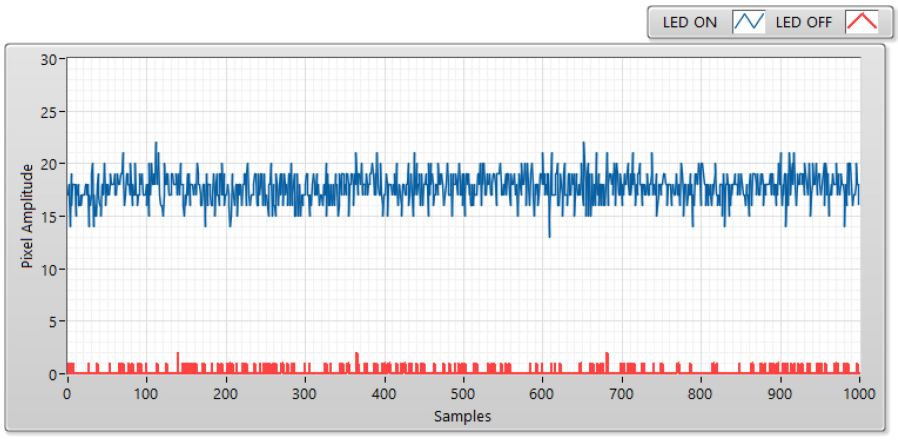

Fig. 7. SNR measurement with rolling shutter camera at 10 m and 50 us exposure time setting.

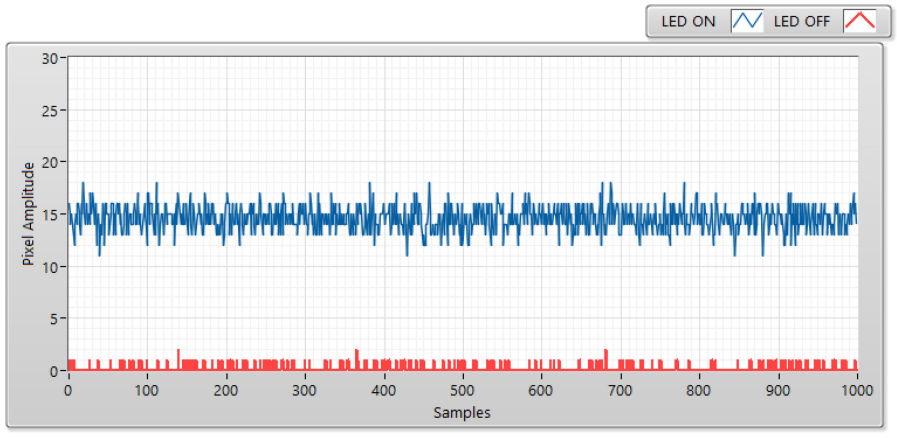

Fig. 8. SNR measurement with rolling shutter camera at 15 m and 50 us exposure time setting.

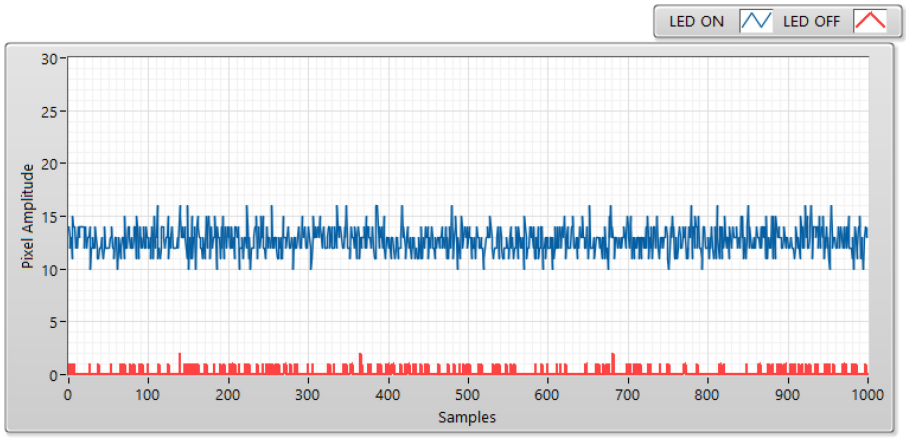

Fig. 9. SNR measurement with rolling shutter camera at 20 m and 50 us exposure time setting.

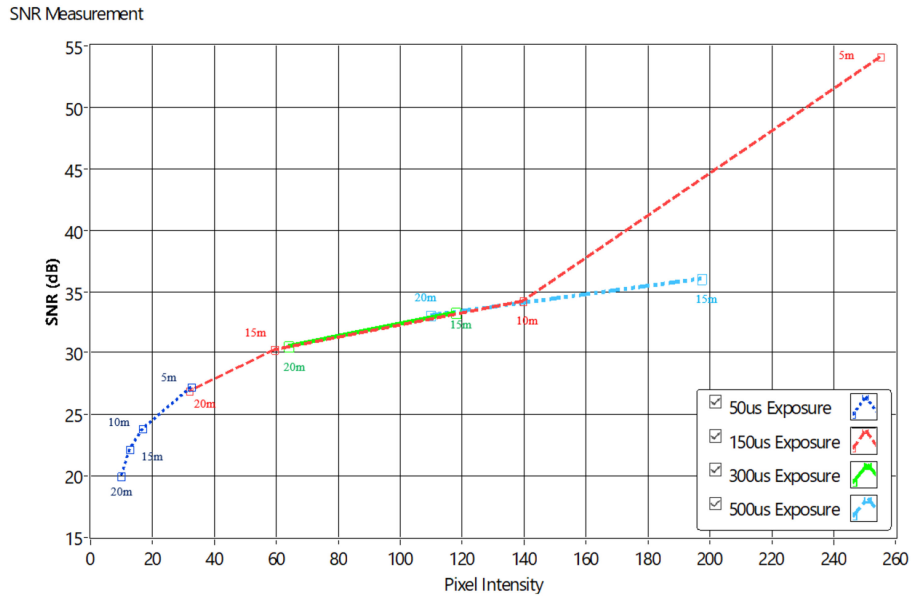

Fig. 10. Measurement result of pixel SNR versus pixel intensity.

Fig. 10 displays the relationship between pixel SNR and pixel intensity in different cases of exposure time: 50 us, 150 us, 300 us, 500 us. The SNR, or E_b/N_0, has been measured based on the change of exposure time and distance. Perceptibly, the exposure time has a substantial impact on the SNR. The image sensor operates as a low-pass filter; then its greater exposure time will smoothen the high-tone signal. If the exposure time increases, the communication bandwidth will decrease, thus, reducing the total noise power spread over the bandwidth. This proves that if the exposure time is set longer, the SNR result is higher.

In summary, the Light of Sight link always guarantees the minimum SNR of 10 dB required for BER lower than 10^{-4} with Single-Carrier Modulation. The SNR can be increased to greater than 35 dB by controlling the exposure time of the rolling-shutter camera. However, the decrease in communication bandwidth must be carefully considered. Besides, the higher exposure time will increase the probability of fuzzy states of LEDs. To mitigate the higher ratio of fuzzy states, OFDM must have Forward Error Correction or a smart decoding algorithm (Artificial Intelligence decoder).

5.3 BER Estimation for Optical-OFDM Methods

In Optical-Orthogonal Frequency-Division Multiplexing (O-OFDM), the symmetric clipping process should be performed in DCO-OFDM [22]. Besides that, ACO-OFDM systems should be applied to the bias clipping at the top of the signal to minimize error.

We defined that K is the attenuation factor of the clipping process, and β_{bottom}, β_{top} are the top-clipping and the bottom clipping levels. In [23], [24], we have the equation:

$$K = \frac{Cov(s, \psi(s))}{\sigma^2} = Q(\beta_{bottom}) - Q(\beta_{top}) \tag{16}$$

where Cov[.] is the covariance operator, σ^2 is the variance of signal s, and $\psi(.)$ is the normalized nonlinear transfer function.

The bit error rate performance of M-QAM O-OFDM can be expressed as [29]:

$$BER = \frac{4(\sqrt{M}-1)}{\sqrt{M}\log_2(M)} Q\left(\sqrt{\frac{3\log_2(M)}{M-1}\Gamma_{b(elec)}}\right) + \frac{4(\sqrt{M}-2)}{\sqrt{M}.\log_2(M)} Q\left(3\sqrt{\frac{3\log_2(M)}{M-1}\Gamma_{b(elec)}}\right) \tag{17}$$

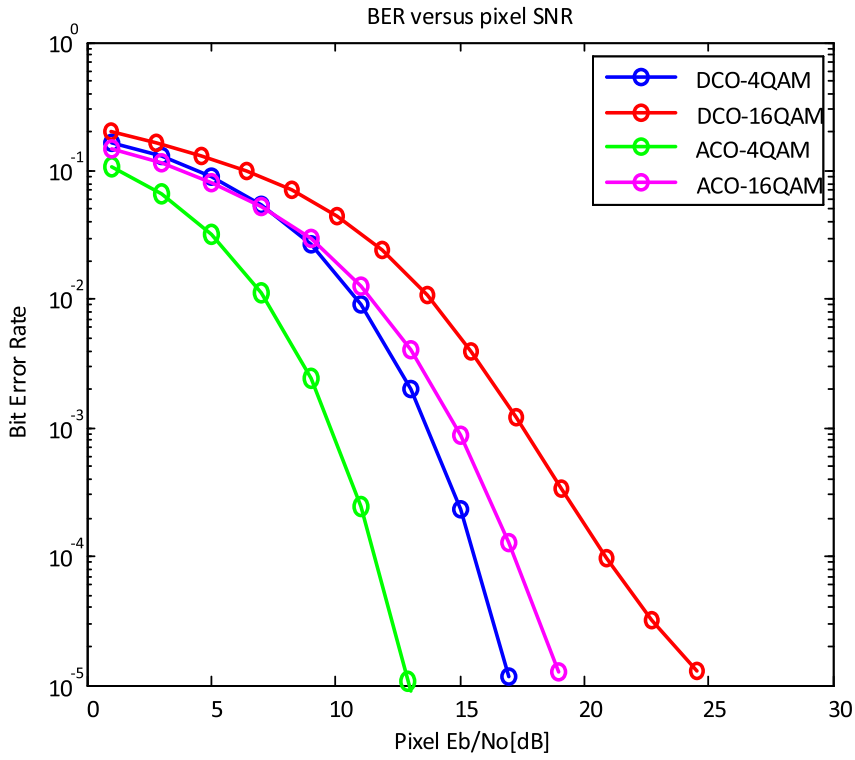

Fig. 11. Simulation bit error rate per Eb/N0 of DCO-OFDM and ACO-OFDM schemes.

where M is the number constellation of symbol QAM. $\Gamma_{b(elec)}$ is the receiver electrical SNR per bit on enabled subcarriers in M-QAM DCO-OFDM and is defined as the following:

$$\Gamma_{b(elec)} = \frac{K^2 P_{b(elec)}/G_B}{\sigma_{clip}^2 + \frac{G_B \sigma_{AWGN}^2}{g_{h(opt)}^2 G_{DC}}} = \frac{K^2}{\frac{G_B \sigma_{clip}^2}{P_{b(elec)}} + \frac{G_B \gamma_{b(elec)}^{-1}}{g_{h(opt)}^2 G_{DC}}} \tag{18}$$

where $\gamma_{b(elec)} = E_b/N_0$ is the electrical SNR per bit; σ_{clip}^2 is the clipping noise variance; G_{DC} is the attenuation of the electrical signal power; $g_{h(opt)}$ is the optical path gain coefficient; G_B is the ratio of utilized(for DCO-OFDM, $G = \frac{N-2}{N}$ and N is the number of carriers. For ACO-OFDM, $G_B = 0.5$.

Fig. 11 shows the estimated curve of DCO-OFDM and ACO-OFDM versus pixel E_b/N_0 with bottom and top clipping levels suitable for the implement parameters in the proposed scheme. The graph demonstrates that O-OFDM schemes require a pixel Eb/N0 of at least 25 dB to achieve BER of 10^{-4}. Compared to the theoretical pixel SNR calculation in Fig. 4 and the experimental SNR results in Fig. 10, the proposed scheme can achieve BER of 10^{-4}at distance of 20 m if we control the exposure time suitably. As mention above, the pixel SNR can be increased by setting longer exposure time, but it will narrow down the communication bandwidth then the control of communication bandwidth need be considered carefully.

5.4 Proposed Schemes

In this subsection, we discuss the format of the proposed scheme shown as Fig. 12. To support the compatibility of frame rate variation, every packet can contain many sub-packets, and each sub-packet in the same packet has the same data payload with a Sequence Number (SN). The SN represents the serial number of packets. In reality, we can divide two cases depending on the packet

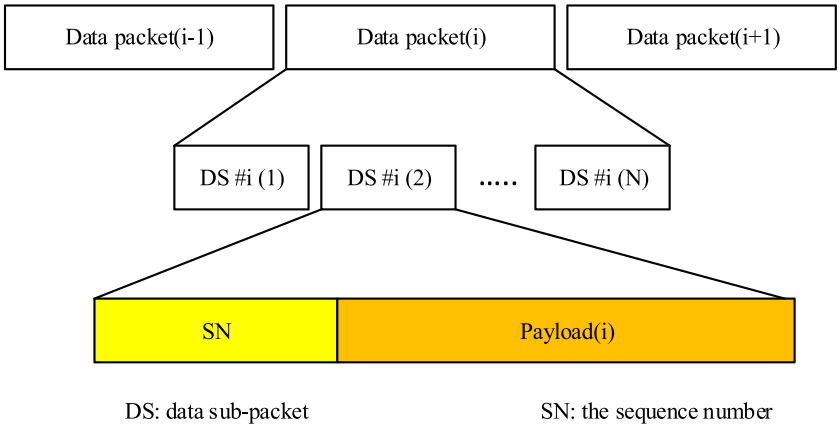

Fig. 12. Proposed data frame structure for Rolling-OFDM system.

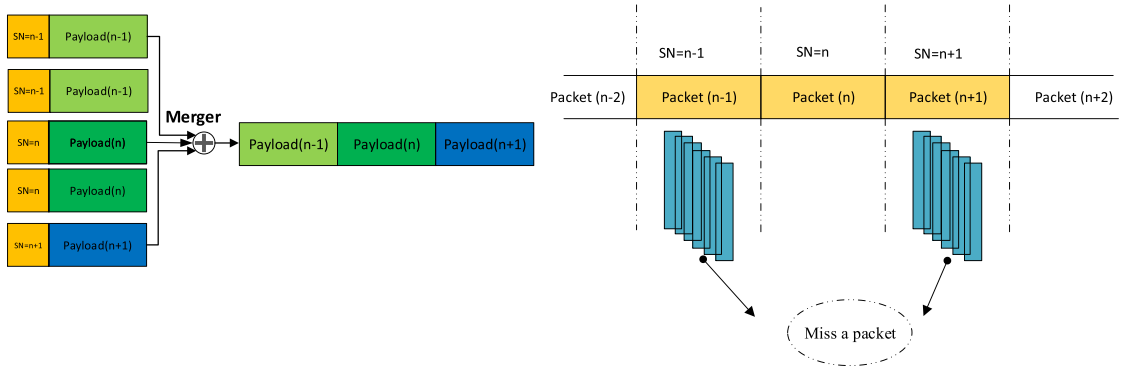

Fig. 13. Merging packet method and detecting missed packets of the proposed schemes.

rate of the transmitter and the frame rate of the camera. Case 1 is called undersampling, in which the frame rate is less than the packet rate of the transmitter (LED). Case 2 is called oversampling, in which the frame rate is many times greater than the packet rate of the transmitter. The packet rate of the transmitter is conceded as the number packet, which carries different payloads across the transmission medium per time period (e.g., 20 packets/s). Our proposed data frame structure contains many data packet frames. Every packet consists of several Data Sub-packets (DS), and each DS consists of payload data and an SN. The SN represents the sequence information of a data packet, which helps a receiver to identify the arrival state of a new payload with a variable rate in the oversampling case and detection of missed payloads in the undersampling case. [25] proposed using 1-bit Ab to synchronize with the oversampling case and 2-bit to synchronize with the undersampling case. It is easy to confuse when decoding in the receiver. Besides that, the 2-bit Ab only detect 3 missing payloads of transmitted packets. Meanwhile, the proposed scheme uses n bits of the Sequence Number. Depending on the parameters of the system, we can change the length of SN. Therefore, the number of detected missing packets will increase depending on the length of SN. Fig. 13 show how to use SN in two main cases: Oversampling and Undersampling.

5.4.1 Oversampling: The Oversampling caused by the frame rate variation of the rolling shutter camera when the frame rate of a rolling-shutter camera becomes many times greater (at least double) than the packet rate of the transmitter, every data packet is sampled at least twice (i.e., two images). At the receiver, we receive the same packet causing confusions of packet merger. To

assist the receiver in reducing the effect of the frame rate variation of the camera, the SN is added to DS. Each packet contains DSs with the same SN, which helps the receiver remove redundant data. When the receiver receives a DS, it will choose which has a compatible SN. The receiver will eliminate consecutive packets with the same SN and choose packets with consecutive SN (n − 1, n, n + 1) to the merger, as shown in Fig. 13.

According to our proposed schemes, each data packet contains several data sub-packets, which is repeated N times so that the data will be not be lost if the camera does not capture in the time between sub-packets. To avoid missed packets when the frame rate of the camera changes, the N value must satisfy the Equation (19):

$$N \geq \frac{(T_{cam})_{\max}}{DS\_length} \tag{19}$$

where *DS_length* is the interval of a DS frame in a packet and T_{cam} is the inter-frame interval of a camera.

5.4.2 Undersampling: Undersampling occurs if the frame rate drops to below the packet rate of the transmitter. In this case, the payload will be lost. The detection of a missed payload using the SN is shown in Fig. 13. If the SN length is long enough, the missed payload can be detected by SN. The data frame achieved from the payload *n – 1* represents the SN as *n – 1*. The next data frame indicates that the SN is *n,* but the actual data frame carries SN *n + 1*. This demonstrates that the payload *n* is missed and the loss is detected by comparing the SN of the two adjacent data sub-packets. However, depending on the length of the SN, a number of different states are generated. For example, if the SN length is 3 bits, seven missing payloads of transmitted packets can be detected by the Sequence Number. The error correction becomes easy if the errors are detected. If two consecutive packets have two non-consecutive SN (n − 1 and n + 1), respectively, the errors happen as shown in Fig. 13.

5.4.3 Data Sub-Packet Length: The rolling rate is an important parameter of the rolling-shutter camera [26]. It is the interval time at which the camera can scan one row of pixels in the image. The number of pixels corresponding to a bit is calculated using the following equation:

$$N_{pixel/bit} = \frac{T_{clock}}{T_{rolling}} \tag{20}$$

According to the novel operation of the rolling-shutter camera and Nyquist's theorem, the condition of the clock rate in the transmitter base on the rolling-shutter speed is $T_{clock} \geq 2.T_{rolling}$.

The OFDM symbol consists of two parts: one part is the payload consisting of useful data, while the other part is the CP. We assumed that the number row of LED in the image is the *LED_size*. The maximum OFDM symbol size or the DS size can be expressed as follows:

$$N_{symbol} \leq \frac{LED\_size}{N_{pixel/bit}} \tag{21}$$

According to Equation (20), (21), we can choose a suitable packet length and clock rate to transmit data using OFDM waveform.

5.5 Implementation for Rolling OFDM

Our experiments have been employed several times with Optical-OFDM schemes and different cameras to verify the frame variation effect. The SN length has been chosen suitably for the asynchronous process. Asynchronous decoding, the detection of a missing part, and the merging data technique are shown in Fig. 13. Besides, some experimental results and parameters are depicted in Table 2. The experiments of the OFDM system are employed with a PointGrey rolling-shutter camera; the frame rate variation of this camera has been calculated as fluctuating between 20 fps and 30 fps. The experimental setup is illustrated in Figs. 14, and 15 shows the OFDM waveform of the receiving camera.

TABLE 2
Rolling-OFDM System Parameters

Tx Side		
Optical clock rate	19.448 kHz	43.413 kHz
The number of OFDM symbol	64	128
FEC	RS(15,11)	
Packet rate	20 packet/s	
LED type	12V, 2.5W	
Rx Side		
Camera type	PointGrey rolling shutter camera	
Camera frame rate	60fps	
Throughput		
Uncoded bit rate	1.280 kbps	2.560 kbps
Code bit rate	0.938 kbps	1.877 kbps

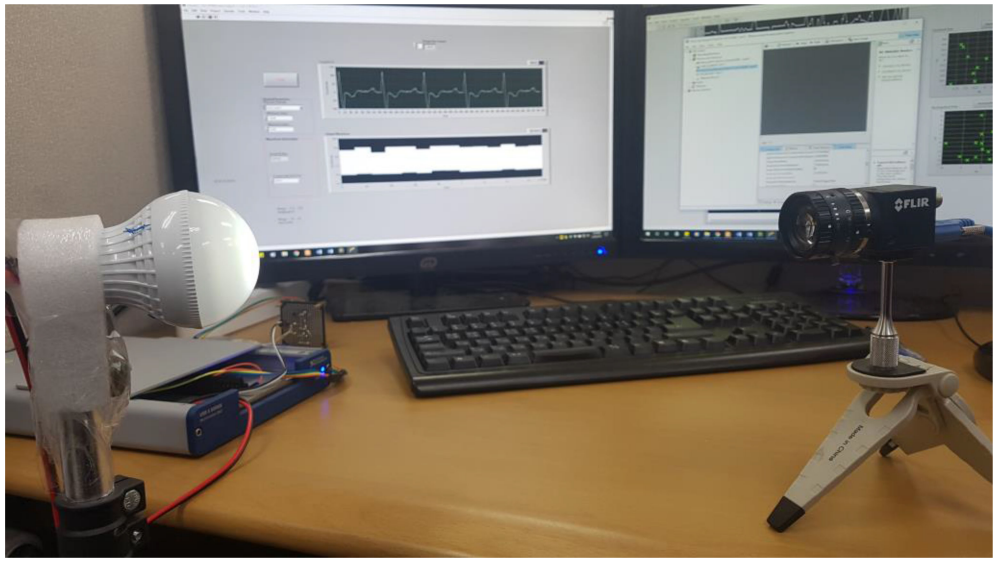

Fig. 14. Setup rolling shutter-OFDM.

Table 2 shows experimental results, which have been conducted several times with some difference in modulation frequencies. The data has been added with the desired SN for the asynchronous packet. Fig. 13 depicts the data merging technique and detecting loss technique. Additionally, the experimental results include numerous modulation frequencies for different symbol lengths (64 bit and 128 bit) to evaluate the performance of the system. The Table shows that 1.280 kbps is achieved when the symbol length is 64 bit and 2.560 kbps when the symbol length is 128 bit. As mentioned above, if the length of the packet is greater, the data rate is better, but the trade-off between the LED size in the image and the data rate must be carefully considered.

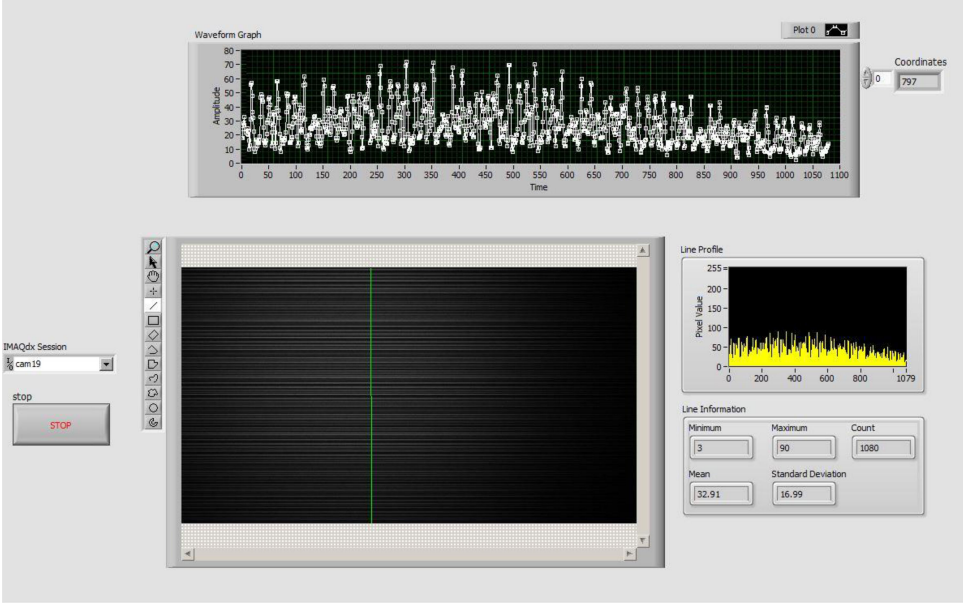

Fig. 15. Rx interface.

6. Conclusion

This paper proposed a rolling-OFDM scheme using in Optical Camera Communication. The proposed frame structure using the Sequence Number (SN) can mitigate the effect of frame rate variation, which is present in rolling-shutter cameras for both the oversampling and undersampling prototype. By using the SN, the detection of the loss payload is resolved with a high-speed transmission link. Besides, the merging of packets from images by using SNs to recover a complete payload is also novelty proposed in this paper. However, the trade-off between transmitted distance and the data rate must be considered. The longer the distance will be, the smaller the size of the LED on an image, which can lead to reduced data per image. Hence, we can appropriately choose the length of the OFDM symbol to increase the performance and data rate of the system.

By inserting an SN on a sub-packet, we can merge some sub-packets from another image to complete the packet. By this method, the error of lost data also is detected due to non-sequential SNs. The possible solution for the trade-off between distance and data rate can be resolved by using zoom modulation in the rolling-shutter camera or by using larger LED in the transmission side to improve the transmission distance without reducing the data rate.

Finally, the results of SNR measurements are shown with different distances to confirm that the proposed OFDM waveform is feasible in a real environment.

References

[1] R. Sridhar, D. Richard, and L. Sang Kyu, "IEEE 802.15.7 visible light communication: Modulation and dimming support," *IEEE Commun. Mag.*, vol. 50, no. 3, pp. 72–82, Mar. 2012.

[2] S. Nikola, J. Volker, J. Yeong Min, and L. Q. John, "An overview on high-speed optical wireless/light communications," 2017. [Online]. Available: https://mentor.ieee.org/802.11/dcn/17/11-17-0962-02-00lc-an-overview-on-high-speed-optical-wireless-light-communications.pdf. Accessed on: 2018.

[3] IEEE standard for local and metropolitan area networks-part 15.7: Short-range wireless optical communication using visible light, IEEE Std 802.15.7-2011, 2011.

[4] T. Nguyen *et al.*, "Current status and performance analysis of optical camera communication technologies for 5G networks," *IEEE Access*, vol. 5, pp. 4574–4594, 2017.

[5] T. Nguyen, A. Islam, T. Yamazato, and Y. M. Jang, "Technical issues on IEEE 802.15.7m image sensor communication standardization," *IEEE Commun. Mag.*, vol. 56, no. 2, pp. 213–218, Feb. 2018.

[6] T. Nguyen, M. D. Thieu, and Y. M. Jang, "2D-OFDM for optical camera communication: Principle and implementation," *IEEE Access*, vol. 7, pp. 29405–29424, 2019.
[7] L. Hanzo, M. Munster, B. Choi, and T. Keller, "OFDM and MC-CDMA for broadband multi-user communications," *WLANs and Broadcasting*. New York, NY, USA: Wiley, 2003.
[8] H. Haas, L. Yin, Y. Wang, and C. Chen, "What is LiFi," *J. Lightw. Technol.*, vol. 34, no. 6, pp. 1533–1544, Mar. 2016.
[9] F. A. Pinto-Benel, M. Blanco-Velasco, and F. Cruz-Roldán, "Throughput analysis of wavelet OFDM in broadband power line communications," *IEEE Access*, vol. 6, pp. 16727–16736, 2016.
[10] H. Hosseini, "Wavelet packet-based multicarrier modulation for cognitive UWB systems," 2010.
[11] W. Huang, C. Gong, and Z. Xu, "System and waveform design for wavelet packet division multiplexing-based visible light communication," *J. Lightw. Technol.*, vol. 33, no. 14, pp. 3041–3051, Jul. 2015.
[12] J. Volker, "HHI High-rate PD communication proposal," 2016. [Online]. Available: https://mentor.ieee.org/802.15/dcn/16/15-16-0016-03-007a-proposal-for-tg7r1-high-rate-pd-communications.docx. Accessed on: 2018.
[13] T. Dobroslav, and S. Nikola, "PureLiFi Low-bandwidth PHY and MAC proposal," 2016. [Online]. Available: https://mentor.ieee.org/802.15/dcn/16/15-16-0363-00-007a-text-input-lifi-low-bandwidth-phy-and-mac-d0.docx. Accessed on: 2018.
[14] J. Zhou *et al.*, "Low-PAPR layered/ enhanced ACO-SCFDM for optical wireless communications," *IEEE Photon. Technol. Lett.*, vol. 30, no. 2, pp. 165–168, Jan. 2018.
[15] S. D. Dissanayake and J. Armstrong, "Comparison of ACO-OFDM, DCO-OFDM and ADO-OFDM in IM/DD systems," *J. Lightw. Technol.*, vol. 31, no. 7, pp. 1063–1072, Apr. 2013.
[16] M. R. H. Modal, K. R. Panta, and J. Armstrong, "Performance of two dimensional asymmetrically clipped optical OFDM," in *Proc. IEEE Globalcom Workshop Opt. Wireless Commun.*, 2010, pp. 995–999.
[17] S. M. Sajad Sadough, M. M. Ichir, P. Duhamel, and E. Jaffrot, "Wavelet-based semiblind channel estimation for ultra wideband OFDM systems," *IEEE Trans. Veh. Technol.*, vol. 58, no. 3, pp. 1302–1314, Mar. 2009.
[18] M. N. Suma, S. V. Narasimhan, and B. Kanmani, "Orthogonal frequency division multiplexing peak-to-average power ratio reduction by best tree selection using coded discrete cosine harmonic wavelet packet transform," *IET Commun.*, vol. 8, no. 11, pp. 1875–1882, Jul. 2014.
[19] "IEEE 1901-2010 standard for broadband over power line networks: Medium access control and physical layer specifications, IEEE-Staandard 1901, 2010.
[20] X. Dong W.-S. Lu, and A. C. K. Soong, "Linear interpolation in pilot symbol assisted channel estimation for OFDM," *IEEE Trans. Wireless Commun.*, vol. 6, no. 5, pp. 1910–1920, May 2007.
[21] R. D. Roberts, "Intel proposal in IEEE 802.15.7r1," 2016. [Online]. Available: https://mentor.ieee.org/802.15/dcn/16/15-16-0006-01-007a-intel-occ-proposal.pdf. Accessed on: August 2018.
[22] S. Dimitrov, S. Sinanovic, and H. Haas, "A comparison of OFDM based modulation schemes for OWC with clipping distortion," in *Proc. 2nd IEEE Workshop Opt. Wireless Commun.*, 2012, pp. 787–791.
[23] S. Randel, F. Breyer, S. C. J. Lee, and J. W. Walewski, "Advanced modulation schemes for short-range optical communications," *IEEE J. Sel. Topics Quantum Electron.*, vol. 16, no. 5, pp. 1280–1289, Sep./Oct. 2010.
[24] S. Dimitrov S. Sinanovic, and H. Haas, "Clipping noise in OFDM based optical wireless communication systems," *IEEE Trans. Commun.*, vol. 60, no. 4, pp. 1072–1081, Apr. 2012.
[25] T. Nguyen *et al.*, "Design and implement of a novel compatible encoding scheme in the time domain for image sensor communication," *Sensor J.*, vol. 16, 2016, Art. no. 736.
[26] H. Nguyen *et al.*, "The impact of camera parameters on optical camera communication," in *Proc. Int. Conf. Artif. Intell. Inf. Commun.*, 2019, pp. 526–529.